Phonon interaction of single excitons and biexcitons

F. Gindele, K. Hild, W. Langbein, and U. Woggon

Institut für Physik, Universität Dortmund, D-44221 Dortmund, Germany

(Received 11 February 1999)

The exciton-phonon coupling of a single zero-dimensional exciton is studied in epitaxially grown $CdSe/Zn_{1-x}Cd_xSe$ quantum dot structures by analyzing its linewidth and phonon-assisted recombination. The single excitons do not couple to only a single phonon mode, but to a distribution of phonons, here consisting of the zone-center ZnSe longitudinal optic (LO) phonon and of mixed modes with an energy statistics centered between the ZnSe and CdSe LO phonon. Both exciton and corresponding biexciton reveal LO-phonon replica intensities of $\sim 3\%$ of the respective zero-phonon emission. These similar LO-phonon coupling strengths are evidence of a reduced polarity of the exciton states within the biexciton as the result of exciton-exciton correlation. [S0163-1829(99)50128-8]

Optical spectroscopy on single, zero-dimensional excitons is presently a fascinating new field because of the possible observation of discrete quantum states without the effect of inhomogeneous broadening. These measurements are feasible by the use of new experimental techniques with high spatial resolution and high sensitivity, and allow the study of the electronic properties of individual quantum dots. The linewidth,[1–3] the internal fine structure due to exchange interaction,[3,4] the formation of biexcitons,[5,6] and excited states[3,5,7] are discussed. The phonon interaction of single, zero-dimensional excitons and biexcitons has not been analyzed yet, probably because most of the experimental studies investigated III-V materials for which the polar phonon coupling is considerably smaller than in II-VI materials. Since the phonon replica are rather weak, they are easily covered by a high density of single exciton lines or the formation of charged excitons[8] and biexcitons.[5–7]

In bulk II-VI semiconductors, the free exciton is strongly coupled to longitudinal optic (LO) phonons, due to the polar Fröhlich coupling, in which the optically excited electronic charge distribution couples via the Coulomb interaction to the charge density induced by the vibrational motion of the lattice atoms. Assuming that the bulk phonon properties are maintained in a quantum dot, the actual strength of the polar coupling depends on the radial distribution of the wave functions considered for the confined electrons and holes. For an ideal quantum dot with spherical and infinitely high barriers, a reduction of the coupling to LO phonons is predicted since the single-particle wave functions of electrons and holes are identical, and no difference in their charge distributions exists.[9] Furthermore, as the result of quantum confinement, a significant increase of the coupling to low-energy acoustic phonons together with a change in the phonon energies itself is discussed both experimentally and theoretically.[10–13] Analyzing experimental data, a qualitative discussion can be made in terms of the Huang-Rhys parameter,[14] which describes the intensity ratio between the zero-phonon line and the corresponding higher phonon satellites in absorption, luminescence, or Raman experiments. For CdSe quantum dots embedded in glasses or organic matrices, Raman spectra show intensity ratios between the first and the second satellite in the range of 3:1 up to 5:1, resulting in a Huang-Rhys parameter around 0.2.[15–17] In these nanocrystals, modifications in the surface structure give various reasons for changes in the charge distribution of electron and hole, and

consequently for changes in the polar coupling strength. The experimentally observed large coupling to LO phonons can be modeled in theory by mechanisms giving rise to differences in the radial parts of the wave functions, such as coupled valence bands and modifications in the hole mass, differences in the dielectric constants between dot and barrier or an extra charge within the dot.[18–20] In the surface-stabilized or matrix-embedded spherical II-VI nanocrystals studied until now, the various extrinsic reasons for changes in the charge distribution of electron and hole give rise to a rather complicated picture of the coupling strength, strongly dependent on sample properties. In contrast, epitaxially grown quantum dots are embedded in semiconducting barrier materials, thus providing an electronically well-defined interface without additional surface states.

In this paper we study epitaxially grown $CdSe/Zn_{1-x}Cd_xSe$ quantum structures. To isolate single excitons, we employ high spatial resolution using mesa structures prepared by electron-beam lithography.[1,4,21] Here, a mesa can be selected for which all phonon-assisted processes detected in photoluminescence (PL) start from a single, zero-dimensional exciton.

The investigated sample consists of a nominally 3 monolayer (ML) thick CdSe layer grown by migration enhanced epitaxy, embedded between a 50-nm ZnSe buffer layer and a 20-nm cap layer. Details of the growth procedure can be found in Refs. 22 and 23. Analysis of the lattice image obtained by high-resolution transmission electron microscopy reveals the formation of CdSe islands of about 10-nm lateral size due to strain-induced accumulation of Cd within a 8-ML-thick mixed $Zn_{1-x}Cd_xSe/ZnSe$ quantum well. The three-dimensional confinement of the excitons in these islands is demonstrated in photoluminescence (PL) and PL-excitation spectroscopy.[24]

From this structure, optically active mesa structures are prepared,[4] and single zero-dimensional excitons and biexcitons can be observed.[6] The average dot densities in the epitaxially grown structures[4,25–28] are 10^{10} to 10^{11} cm^{-2}, and thus mesa sizes below $(100~\text{nm})^2$ contain only a few dots. The distance between individual mesas on the sample was $200~\mu$m, enough to ensure the suppression of PL from other mesas. The sample is mounted in a cold-finger Helium flow cryostat, and excited by the 488-nm line of an Ar$^+$ laser focused to a spot size of $\approx 80~\mu$m. The PL is collected by an 0.4 numerical aperture (NA) objective with 1-μm resolution,
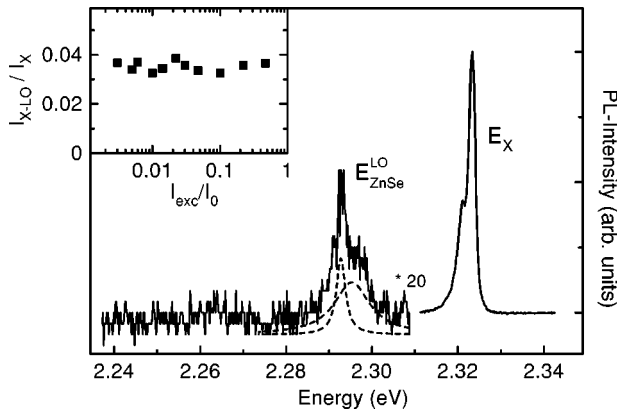
FIG. 1. PL spectrum of a single exciton E_X measured from a 50×50-nm^2 mesa at an intensity of $I_{exc} = 12$ W/cm^2. The inset shows the intensity ratio between the LO-phonon replica and the zero-phonon line I_{X-LO}/I_X vs excitation intensity; $I_0 = 4.2$ kW/cm^2, $T = 5$ K.

dispersed by a 0.46-m spectrometer with a 1200 l/mm grating in first order, and detected by a liquid-nitrogen cooled charge couple device camera.

We investigate here a (50-nm)^2 square mesa structure, showing only one single excitonic transition. Figure 1 shows the emission spectrum of the mesa at an excitation intensity of 12 W/cm^2 using an integration time of 1200 s. Even at this low excitation, the line shape of the exciton emission is not a pure Lorentzian, but shows a substructure. We exclude exchange splitting as a possible explanation since the corresponding polarization dependence could not be found in the spectrum of that selected single exciton. Presumably the exchange splitting energy is very small and covered by a special type of time-dependent inhomogeneous broadening caused by local electrical fields due to carrier trapping. Indications for such a process are small drifts of the energy position (~ 0.9 meV) of the single exciton line and the intensity dependence of its energy maximum, which will be discussed below. Similar effects have been observed, e.g., for CdSe nanocrystals.[2]

The satellite peak below the exciton emission is attributed to LO-phonon-assisted recombination of the single exciton. This structure can be decomposed into a narrow peak 31 meV below the zero-phonon line and of similar width (1.8 meV), and a broad background band of 9-meV width peaking around 28 meV below the zero-phonon emission. The first peak corresponds to the ZnSe zone center LO phonon, while the broad background lies mainly between the ZnSe and the CdSe LO-phonon energy. This shows that the localized exciton wave function couples to both ZnSe and CdSe–like LO phonons. While the ZnSe bulk LO phonon is strongly pronounced due to the surrounding binary ZnSe barriers, the phonons involving Cd atoms are of varying energy due to the microscopic disorder of the Cd distribution on the cation sublattice. The energy distribution also involves phonons with energies below the CdSe zone-center LO phonon. Keeping in mind the negative LO-phonon dispersion, this indicates the localization of the related phonons. The line shape of the LO-phonon replica demonstrates that a single exciton state does not couple to only a *single phonon*. The phonon energies excited via the polar coupling are distributed according to the local Cd distribution probed by the
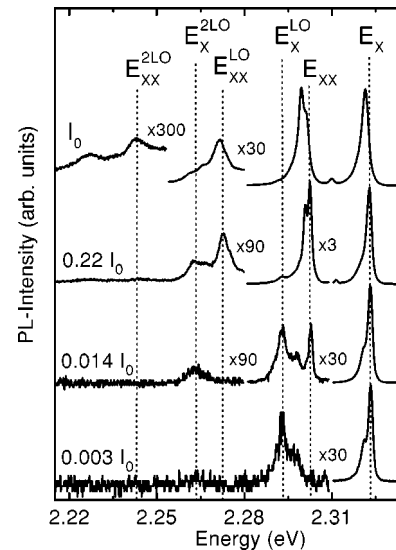
FIG. 2. Intensity dependence of the single exciton spectra E_X of the same mesa as for Fig. 1. With increasing intensity the first LO-phonon replica E_X^{LO} is covered by the biexciton E_{XX} and its LO-phonon replica E_{XX}^{LO}. Additionally, the second replica E_X^{2LO} and E_{XX}^{2LO} emerge. $I_0 = 4.2$ kW/cm^2, $T = 5$ K.

exciton wave function, and contribute to the LO-phonon replica according to their coupling strength.

The intensity ratio between the zero-phonon exciton emission and the LO-phonon replica, considered here as a measure for the coupling strength, amounts to 0.035. All the ratios observed for similar single exciton transitions are in the range of 0.015–0.05, values much smaller than the average of 0.5 found for CdSe nanocrystals.[2] This shows that the localized excitons in the epitaxially grown dots have a smaller polarity of the excitonic wave function, probably due to the smaller dielectric confinement and the well-defined surface structure. The measured ratio is not sensitive to effects of higher excitation density (see inset of Fig. 1), i.e., exciton-exciton interaction or electric field effects do not influence the charge distribution significantly.

Figure 2 shows the evolution of the PL for increasing excitation intensity. The spectra are normalized to the zero-phonon exciton line. At $0.014 I_0$, the better signal-to-noise ratio allows the observation of the second LO-phonon replica E_X^{2LO} of the localized exciton E_X. A peak labeled E_{XX} appears below the exciton, showing an intensity proportional to the square of the excitation intensity. We assign this peak to the emission of the biexciton-exciton transition. Its energy separation from the exciton of 20 meV is in agreement with the biexciton binding energy obtained by two-photon absorption and four-wave mixing experiments,[29] and magnetophotoluminescence.[6] Together with the biexciton E_{XX}, a satellite peak one ZnSe-LO-phonon energy below E_{XX} labeled E_{XX}^{LO} emerges, which we attribute to the first LO-phonon replica of the biexciton emission. The line shape of the E_{XX}^{LO} peak is slightly asymmetric indicating a similar interaction with LO phonons of varying energy as observed for the exciton. To our knowledge, phonon coupling to single zero-dimensional biexcitons has not been reported until now. The intensity ratio between the biexciton replica and E_{XX} is ~ 0.032, close to the value obtained for the exciton emission. From that result it can be concluded that the polarity of the
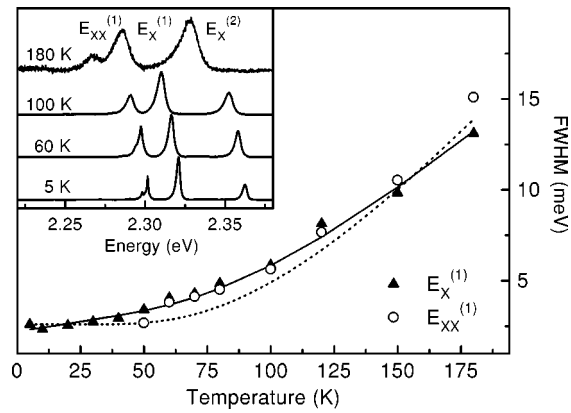
FIG. 3. Temperature dependence of the exciton and biexciton linewidth. In the inset the PL spectra are plotted showing a pair of exciton and biexciton lines, $E_X^{(1)}$ and $E_{XX}^{(1)}$, and a second exciton $E_X^{(2)}$ separated in energy by 42 meV. The dotted line is a fit based solely on the Bose statistics ($\hbar\omega_{LO} = 28$ meV), the solid line shows the fit after involving acoustic phonons (see text).

wave function of the localized biexciton is not twice the exciton polarity. Obviously, the four-particle correlation gives rise to a distinct deformation of the uncorrelated exciton wave functions, reducing their polarity that results in a repulsive interaction between the excitons. This strong reduction is a consequence of the largely enhanced biexciton binding energy (~ 20 meV compared to 4 meV in bulk CdSe) by the 3D-quantum confinement, which allows for a strong influence of the biexciton binding on the single exciton wave functions.

Next, we discuss the intensity dependence of the line shape of the localized exciton itself. As can be seen in Fig. 2, the peak position slightly shifts to lower energies with increasing excitation accompanied by a small increase in line broadening. This behavior can be ascribed to (i) an increase in lattice temperature of the sample or (ii) the formation of stronger electric fields inside the sample by charge trapping on the surface or interfaces. Such fields lead to a quantum-confined Stark effect, shifting the exciton to lower energies quadratically in the field strength. This also explains the low-energy tail of the emission, instead of a symmetric broadening. For high excitation intensities, sometimes sudden changes of the line shape are observed, shifting the emission by about the biexciton binding energy to lower energies, and broadening the line strongly. We interpret this as due to trapping of an electron or hole inside the dot, leading to the formation of charged excitons (trions),[8] which are observed, e.g., in GaAs, CdTe, and ZnSe quantum wells with binding energies comparable to the biexciton binding energy.

Finally, the phonon coupling is studied analyzing the temperature-dependent line broadening of localized excitons. Figure 3 shows an example for a mesa structure which contains one localized exciton $E_X^{(1)}$ along with its biexciton $E_{XX}^{(1)}$

and a second localized exciton $E_X^{(2)}$ separated in energy by about 42 meV. In the case of several differently localized excitons, not only the line shape changes with temperature, but also the intensity ratios, as can be seen in the inset of Fig. 3. This fact indicates the thermal depopulation of the lowest exciton state in favor of the population of the next higher state. In Fig. 3 the full width at half of maximum (FWHM) of the PL lines is plotted for both the exciton and the biexciton as a function of temperature. Below $T = 50$ K only small changes in the linewidth are observed. A change in slope is detected between 30 K and 70 K. When fitting the curves by an activation energy based on the Bose statistics for LO phonons with an average energy of 28 meV (dotted line), as observed in the phonon replica (Fig. 1), the broadening is underestimated at temperatures around 100 K. This indicated the importance of acoustic-phonon-induced broadening. This broadening is in quantum dots with missing final states of suitable energy not due to a real phonon absorption, but due to a phonon scattering. It is enhanced by the strong three-dimensional confinement, enlarging the range of quasi-momentum conservation.[10] Taking into account this acoustic phonon pure dephasing of 20 μeV/K, as predicted for a CdSe quantum dot of 4-nm radius,[10] the experimental temperature dependence is well reproduced.

Surprisingly, the temperature-dependent line broadening of the biexciton transition is not significantly different from that of the exciton. This result is a clear hint to the correlation of exciton and biexciton scattering. In case of an uncorrelated scattering, a sum of exciton and biexciton scattering rate is expected, which should be distinctly higher than the observed linewidth. Such a correlated scattering is also found in $In_xGa_{1-x}As$ quantum wells.[30]

Summarizing, we have found that three-dimensional confinement can result in a small polar coupling strength, in agreement with earlier theoretical predictions.[9] Investigating a single zero-dimensional exciton, the problem of inhomogeneous broadening is avoided and the phonon coupling of single excitons and biexcitons has been observed. A coupling parameter of 0.035 for the exciton and 0.032 for the biexciton is found, showing a strong correlation of the two excitons within the biexciton. The phonon replica consist of a band of LO-phonon energies demonstrating that the single exciton couples to a variety of phonon modes, not to a single one. The contributing phonon energies have parts from the zone-center LO phonon of ZnSe, and from a distribution centered between the ZnSe and the CdSe LO-phonon energy resulting from the microscopic disorder of Cd on the cation sublattice.

[1] J.-Y. Marzin, J. M. Gerard, A. Izrael, D. Barrier, and G. Bastard, Phys. Rev. Lett. **73**, 716 (1994).

[2] S.A. Empedocles, D.J. Norris, and M.G. Bawendi, Phys. Rev. Lett. **77**, 3873 (1996).

[3] D. Gammon, E.S. Snow, B.V. Shanabrook, D.S. Katzer, and D. Park, Phys. Rev. Lett. **76**, 3005 (1996).

[4] T. Kümmell, R. Weigand, G. Bacher, A. Forchel, K. Leonardi, D. Hommel, and H. Selke, Appl. Phys. Lett. **73**, 3105 (1998).

[5] A. Kuther, M. Bayer, A. Forchel, A. Gorbunov, V.B. Timofeev, F. Schäfer, and J.P. Reithmaier, Phys. Rev. B **58**, R7508 (1998).

[6] V.D. Kulakovskii, G. Bacher, R. Weigand, T. Kümmell, A. Forchel, E. Borovitskaya, K. Leonardi, and D. Hommel, Phys. Rev. Lett. **82**, 1780 (1999).

[7] H. Kamada, H. Ando, J. Temmyo, and T. Tamamura, Phys. Rev. B **58**, 16 243 (1998).

[8] K. Kheng, R.T. Cox, Y. Merle d'Aubige, F. Bassani, K. Saminadayar, and S. Tatarenko, Phys. Rev. Lett. **71**, 1752 (1993).

[9] S. Schmitt-Rink, D.A.B. Miller, and D.S. Chemla, Phys. Rev. B **35**, 8113 (1987).

[10] T. Takagahara, Phys. Rev. Lett. **71**, 3577 (1993).

[11] D.M. Mittleman, R.W. Schoenlein, J.J. Shiang, V.L. Colvin, A.P. Alivisatos, and C.V. Shank, Phys. Rev. B **49**, 14 435 (1994).

[12] U. Woggon, F. Gindele, O. Wind, and C. Klingshirn, Phys. Rev. B **54**, 1506 (1996).

[13] Huaxiang Fu, V. Ozolins, and A. Zunger, Phys. Rev. B **59**, 2881 (1999).

[14] K. Huang and A. Rhys, Proc. R. Soc. London, Ser. A **204**, 406 (1954).

[15] M.C. Klein, F. Hache, D. Ricard, and C. Flytzanis, Phys. Rev. B **42**, 11 123 (1990).

[16] A.P. Alivisatos, T.D. Harris, P.J. Caroll, M.L. Steigerwald, and L.E. Brus, J. Chem. Phys. **90**, 3463 (1989).

[17] R. Rosetti, S. Nakahara, and L.E. Brus, J. Chem. Phys. **79**, 1086 (1983).

[18] S. Nomura and T. Kobayashi, Phys. Rev. B **45**, 1305 (1992).

[19] L. Banyai, P. Gilliot, Y.Z. Hu, and S.W. Koch, Phys. Rev. B **45**, 14 136 (1992).

[20] Al. L. Efros, Superlattices Microstruct. **11**, 167 (1992).

[21] M. Illing, G. Bacher, T. Kümmell, A. Forchel, T.G. Andersson, D. Hommel, B. Jobst, and G. Landwehr, Appl. Phys. Lett. **67**, 124 (1995).

[22] K. Leonardi, H. Heinke, K. Ohkawa, D. Hommel, H. Selke, F. Gindele, and U. Woggon, Appl. Phys. Lett. **71**, 1510 (1997).

[23] K. Leonardi, H. Heinke, K. Ohkawa, D. Hommel, H. Selke, F. Gindele, and U. Woggon, J. Cryst. Growth **184/185**, 259 (1998).

[24] F. Gindele, U. Woggon, W. Langbein, J.M. Hvam, K. Leonardi, K. Ohkawa, and D. Hommel, J. Cryst. Growth **184/185**, 306 (1998).

[25] S.V. Ivanov, A.A. Toropov, S.V. Sorokin, T.V. Shubina, I.V. Sedove, A.A. Sitnikova, P.S. Kopev, Zh. I. Alferov, H.-J. Lugauer, G. Reuscher, M. Keim, F. Fischer, A. Waag, and G. Landwehr, Appl. Phys. Lett. **74**, 498 (1999).

[26] M. Rabe, M. Lowisch, F. Kreller, and F. Henneberger, Phys. Status Solidi B **202**, 817 (1997).

[27] S.H. Xin, P.D. Wang, Aie Yin, C. Kim, M. Dobrowolska, J.L. Merz, and J.K. Furdyna, Appl. Phys. Lett. **69**, 3884 (1996).

[28] V. Nikitin, P.A. Cromwell, J.A. Gupta, D.D. Awschalom, F. Flack, and N. Samarth, Appl. Phys. Lett. **71**, 1213 (1997).

[29] F. Gindele, U. Woggon, W. Langbein, J.M. Hvam, K. Leonardi, D. Hommel, and H. Selke, in *Proceedings of the ICPS, Jerusalem, 1998*, edited by D. Gershoni (World Scientific, Singapore, 1998).

[30] P. Borri, W. Langbein, J.M. Hvam, and F. Martelli, in *Proceedings of the ICPS, Jerusalem, 1998* (Ref. 29).